Збірник праць Інституту математики НАН України 2016, т. 13, № 3, 266–280

УДК 532.595

Resonant sloshing in a square-base tank due to an angular-and-horizontal periodic forcing*

A. N. Timokha[1,2]

[1] *Institute of Mathematics of NAS of Ukraine, Kyiev;*
[2] *Centre of Excellence "AMOS", Norwegian University of Science and Technology, Trondheim, Norway; atimokha@gmail.com*

Розробляється модальний метод для задачі про коливання рідини у резервуарі квадратного перерізу, який виконує періодичні горизонтальні та кутові рухи малої амплітуди. Аналіз показує, що домінантна хвильова компонента виключно визначається першою гармонікою періодичного збурення. Еквівалентні гармонічні рухи є зворотнопоступального чи еліптичного типу. Вивчено усталені резонансні хвильові режими для таких типів збурення.

Разрабатывается модальный метод для задачи про колебания жидкости в резервуаре квадратного сечения, который совершает периодические горизонтальные и угловые движения малой амплитуды. Анализ показывает, что доминантная волновая компонента исключительно определяется первой гармоникой периодического возбуждения. Эквивалентные гармонические движения являются возвратно-поступательными или эллиптического типов. Изучено установившиеся резонансные волновые режимы для такого типа возмущений.

*The work was partly supported by the Grant № 0112U001015. The author also acknowledges the financial support of the Centre of Autonomous Marine Operations and Systems (AMOS) whose main sponsor is the Norwegian Research Council (Project number 223254–AMOS).

Introduction

The paper [1] originated theoretical studies on resonant sloshing in a square-base tank performing either longitudinal (along parallel walls) or diagonal harmonic excitations with the forcing frequency close to the lowest natural sloshing frequency. A weakly-nonlinear multimodal theory was developed. The results on the steady-state wave regimes were validated by experiments. The forthcoming parts [2] and [3] focused on amplification of the higher natural sloshing modes and the base ratio perturbation. The studies [1–3] were followed up by many researchers who adopted numerical methods [9–11] and their own versions of the multimodal theory [6–8, 12]. New model tests were also done in [7, 10, 11]. The main focus was on investigating the planar, nearly-diagonal (squares-like), swirling and irregular resonant steady-state sloshing. As in [2, 4], the papers [6, 8, 9, 12] also investigated the energy transfer from lower to higher natural sloshing modes. A novelty was an experimental and numerical analysis of the steady-state resonant sloshing for an oblique (neither longitudinal nor diagonal) horizontal harmonic forcing [6, 7, 10, 11].

The present paper suggests an arbitrary periodic (not necessarily harmonic!) combined *surge-sway-roll-pitch periodic* tank motion with a small amplitude and generalises [1] to identify stable and unstable steady-state resonant sloshing regimes. This implicitly implies, that (i) the forcing frequency σ is close to the lowest natural sloshing frequency σ_1, (ii) the two lowest degenerated (Stokes) natural sloshing modes give the dominant asymptotic contribution, and (iii) the secondary resonance phenomena can be neglected and, therefore, the Narimanov-Moiseev asymptotic theory is applicable.

1 Statement

A rigid square base tank is partially filled by a perfect incompressible liquid with the mean depth h. Irrotational liquid flows are assumed. The tank moves with a small amplitude (relative to the base size) by surge, sway, roll, and pitch; the heave and yaw are zeros. The liquid sloshing is considered in the non-inertial coordinate system $Oxyz$ which is fixed with the rigid tank so that Oxy-plane coincides with the mean free surface Σ_0 and Oz passes through the centre of Σ_0. Figure 1 introduces basic notations including the translatory $\boldsymbol{v}_O(t)$ and instant angular $\boldsymbol{\omega}(t)$ velocities of the tank. The free surface $\Sigma(t) : z = f(x, y, t)$ and the absolute velocity

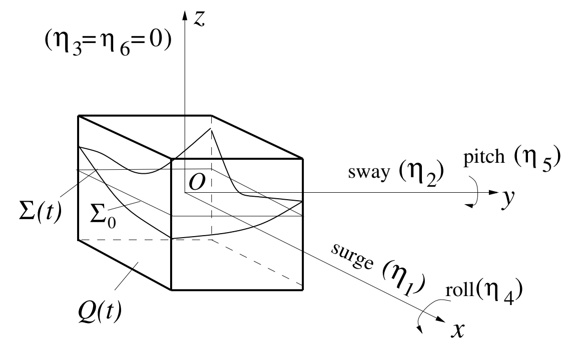

Figure 1. Sketch of a square-base tank which moves periodically by surge, sway, roll, and pitch so that the tank translatory velocity is $\boldsymbol{v}_O(t) = (v_{O1}(t), v_{O2}(t), 0) = (\dot{\eta}_1(t), \dot{\eta}_2(t), 0)$ and the instant angular velocity is $\boldsymbol{\omega}(t) = (\omega_1(t), \omega_2(t), 0) = (\dot{\psi}_1(t), \dot{\psi}_2(t), 0) = (\dot{\eta}_4, \dot{\eta}_5, 0)$. The $Oxyz$ system is rigidly fixed with the tank so that the mean free surface Σ_0 belongs to Oxy and the origin is in the centre of the rectangle Σ_0.

potential $\Phi(x, y, z, t)$ must be simultaneously found from the corresponding free-surface problem or its variational analogy [5]. The task consists of finding an approximate *analytical steady-state solution* of the problem, $f(x, y, t+2\pi/\sigma) = f(x, y, t)$ and $\Phi(x, y, z, t+2\pi/\sigma) = \Phi(x, y, z, t)$, where σ is the circular frequency of the periodic tank motions.

The Narimanov–Moiseev nonlinear multimodal theory of the resonant sloshing is used. This assumes that σ is close to the natural sloshing frequency σ_1 of the two standing Stokes cross-wave modes and these modes are amplified with the lowest asymptotic order $O(\epsilon^{1/3})$ where $\epsilon \ll 1$ (all geometric parameters are scaled by the breadth = width = L_1 so that the tank cross-section becomes a unit square, $h := h/L_1$ and $g := g/L_1$, where g is the gravity acceleration) is associated with the nondimensional forcing amplitude. As explained in Chapters 8 and 9 of [5], the Narimanov–Moiseev theory may fail due to the secondary resonant phenomena whose occurrence in the *square base* tank is expected at critical and small liquid depths as well as when the forcing amplitude increases causing the surface-wave breaking and fragmentations [4]. The modal theory starts with the Fourier (modal) representation

$$f(x, y, t) = \sum_{i,j\geq 0, i+j\neq 0} \beta_{i,j}(t) f_i^{(1)}(x) f_j^{(2)}(y), \tag{1}$$

where $f_i^{(1)}(x)\,f_j^{(2)}(y)$ are the natural sloshing modes and

$$f_i^{(1)}(x)=\cos(\pi i(x+1/2)),\quad f_i^{(2)}(y)=\cos(\pi i(y+1/2)),\quad i\geq 0 \tag{2}$$

are the Stokes modes. Instead of working with the original fully-nonlinear problem, we adopt the weakly-nonlinear approximate (modal) system of ordinary differential equations coupling $\beta_{i,j}(t)$ [1]:

$$\begin{aligned}\ddot a_1+\sigma_{1,0}^2a_1+d_1(\ddot a_1a_2+\dot a_1\dot a_2)+d_2(\ddot a_1a_1^2+\dot a_1^2a_1)+d_3\ddot a_2a_1\\+d_6\ddot a_1b_1^2+\ddot b_1(d_7c_1+d_8a_1b_1)+d_9\ddot c_1b_1+d_{10}\dot b_1^2a_1+d_{11}\dot a_1\dot b_1b_1+d_{12}\dot b_1\dot c_1\\=-P_{1,0}(\ddot\eta_1-S_{1,0}\ddot\eta_5-g\eta_5)=K_x(t),\end{aligned}\tag{3a}$$

$$\begin{aligned}\ddot b_1+\sigma_{0,1}^2b_1+d_1(\ddot b_1b_2+\dot b_1\dot b_2)+d_2(\ddot b_1b_1^2+\dot b_1^2b_1)+d_3\ddot b_2b_1+d_6\ddot b_1a_1^2\\+\ddot a_1(d_7c_1+d_8a_1b_1)+d_9\ddot c_1a_1+d_{10}\dot a_1^2b_1+d_{11}\dot a_1\dot b_1a_1+d_{12}\dot a_1\dot c_1\\=-P_{0,1}(\ddot\eta_2+S_{0,1}\ddot\eta_4+g\eta_4)=K_y(t),\end{aligned}\tag{3b}$$

$$\ddot a_2+\sigma_{2,0}^2a_2+d_4\ddot a_1a_1+d_5\dot a_1^2=0;\qquad \ddot b_2+\sigma_{0,2}^2b_2+d_4\ddot b_1b_1+d_5\dot b_1^2=0,\tag{3c}$$

$$\ddot c_1+\hat d_1\ddot a_1b_1+\hat d_2\ddot b_1a_1+\hat d_3\dot a_1\dot b_1+\sigma_{1,1}^2c_1=0,\tag{3d}$$

$$\begin{aligned}\ddot a_3+\sigma_{3,0}^2a_3+\ddot a_1(q_1a_2+q_2a_1^2)+q_3\ddot a_2a_1+q_4\dot a_1^2a_1+q_5\dot a_1\dot a_2\\=-P_{3,0}(\ddot\eta_1-S_{3,0}\ddot\eta_5-g\eta_5),\end{aligned}\tag{4a}$$

$$\begin{aligned}\ddot c_{21}+\sigma_{2,1}^2c_{21}+\ddot a_1(q_6c_1+q_7a_1b_1)+\ddot b_1(q_8a_2+q_9a_1^2)+q_{10}\ddot a_2b_1+q_{11}\ddot c_1a_1+\\+q_{12}\dot a_1^2b_1+q_{13}\dot a_1\dot b_1a_1+q_{14}\dot a_1\dot c_1+q_{15}\dot a_2\dot b_1=0,\end{aligned}\tag{4b}$$

$$\begin{aligned}\ddot c_{12}+\sigma_{1,2}^2c_{12}+\ddot b_1(q_6c_1+q_7a_1b_1)+\ddot a_1(q_8b_2+q_9b_1^2)+q_{10}\ddot b_2a_1+q_{11}\ddot c_1b_1+\\+q_{12}\dot b_1^2a_1+q_{13}\dot a_1\dot b_1b_1+q_{14}\dot b_1\dot c_1+q_{15}\dot a_1\dot b_2=0,\end{aligned}\tag{4c}$$

$$\begin{aligned}\ddot b_3+\sigma_{0,3}^2b_3+\ddot b_1(q_1b_2+q_2b_1^2)+q_3\ddot b_2b_1+q_4\dot b_1^2b_1+q_5\dot b_1\dot b_2\\=-P_{0,3}(\ddot\eta_2+S_{0,3}\ddot\eta_4+g\eta_4),\end{aligned}\tag{4d}$$

where $\beta_{1,0} = a_1, \beta_{2,0} = a_2, \beta_{0,1} = b_1, \beta_{0,2} = b_2, \beta_{1,1} = c_1, \beta_{3,0} = a_3, \beta_{2,1} = c_{21}, \beta_{1,2} = c_{12}, \beta_{0,3} = b_3$,

$$P_{i,0} = P_{0,i} = \frac{2}{\pi i}\tanh(\pi i h)[(-1)^i - 1],\ S_{i,0} = S_{0,i} = \frac{2}{\pi i}\tanh(\pi i h/2) \quad (5)$$

and $\sigma_1 = \sigma_{0,1} = \sigma_{1,0}$, $\sigma^2_{i,j} = g\pi\sqrt{i^2+j^2}\lambda_{i,j}\tanh(\pi\sqrt{i^2+j^2}h)$. The explicit expressions for the hydrodynamic coefficient and the corresponding tables are given in [1] and [5]. Following [5], we re-denote, the nondimensional generalised coordinates $\eta_i(t) = O(\epsilon) \ll 1$ determining the periodic surge, sway, roll and pitch tank motions.

The modal system (3)–(4) is equivalent to the original free-surface problem within the framework of the Narimanov-Moiseev asymptotic approximation. It makes it possible to analyse steady-state regimes, their stability as well as transient waves. Chapter 9 by [5] outlines other modified weakly-nonlinear modal theories which account for the secondary resonance.

2 Asymptotic steady-state solutions of (3)–(4)

Following [1], we introduce the lowest-order approximation of the steady-state solution

$$a_1 = A\cos\sigma t + \bar{A}\sin\sigma t + o(\epsilon^{1/3});\quad b_1 = \bar{B}\cos\sigma t + B\sin\sigma t + o(\epsilon^{1/3}) \quad (6)$$

responsible for the first two Stokes cross-waves, by $f_1^{(1)}(x)$ and $f_1^{(2)}(y)$. We substitute (6) into (3c), (3d) and (3a), (3b) and (4) to get the second- and third-order terms of the steady-state solution, respectively. Gathering the first Fourier harmonic components in (3) yields a solvability condition appearing as the following system of nonlinear algebraic equations

$$\begin{cases} ①\colon A\big[\Lambda + m_1(A^2+\bar{A}^2) + m_2\bar{B}^2 + m_3B^2\big] + (m_2 - m_3)\bar{A}\bar{B}B = \epsilon_x, \\ ②\colon B\big[\Lambda + m_1(B^2+\bar{B}^2) + m_2\bar{A}^2 + m_3A^2\big] + (m_2 - m_3)\bar{A}A\bar{B} = \epsilon_y, \\ ③\colon \bar{A}\big[\Lambda + m_1(A^2+\bar{A}^2) + m_2B^2 + m_3\bar{B}^2\big] + (m_2 - m_3)A\bar{B}B = \bar{\epsilon}_x, \\ ④\colon \bar{B}\big[\Lambda + m_1(B^2+\bar{B}^2) + m_2A^2 + m_3\bar{A}^2\big] + (m_2 - m_3)\bar{A}AB = \bar{\epsilon}_y \end{cases} \quad (7)$$

with respect to the lowest-order wave amplitudes $A, \bar{A}, B, \bar{B} = O(\epsilon^{1/3})$, where $\Lambda = \bar{\sigma}_1^2 - 1 = \sigma_1^2/\sigma^2 - 1$. The $O(\epsilon)$-order nondimensional amplitude parameters $\epsilon_x, \bar{\epsilon}_x$, ϵ_y and $\bar{\epsilon}_y$ are the first Fourier harmonic components in the right-hand sides of (3a) and (3b)

$$\begin{aligned} \epsilon_x &= \frac{2}{T\sigma^2}\int_0^T \cos\sigma t\, K_x(t)\,\mathrm{d}t; \quad \bar{\epsilon}_x = \frac{2}{T\sigma^2}\int_0^T \sin\sigma t\, K_x(t)\,\mathrm{d}t, \\ \bar{\epsilon}_y &= \frac{2}{T\sigma^2}\int_0^T \cos\sigma t\, K_y(t)\,\mathrm{d}t; \quad \epsilon_y = \frac{2}{T\sigma^2}\int_0^T \sin\sigma t\, K_y(t)\,\mathrm{d}t. \end{aligned} \tag{8}$$

At least one from $\epsilon_x, \bar{\epsilon}_x, \bar{\epsilon}_y$ and ϵ_y should not be zero. *Henceforth,*

1. The Ox-axis direction is chosen to get $\sqrt{\epsilon_y^2+\bar{\epsilon}_y^2} \le \sqrt{\epsilon_x^2+\bar{\epsilon}_x^2} \neq 0$.
2. An appropriate time-phase shift $t := t+\psi_0$ is used to achieve

$$\bar{\epsilon}_x = 0 \text{ and } 0 \le \sqrt{\epsilon_y^2+\bar{\epsilon}_y^2} = \tilde{\epsilon}_y \le \epsilon_x \neq 0. \tag{9}$$

3. The derivation line

$$0 = (\bar{A}\,①-A\,③) - (\bar{B}\,②-B\,④) \equiv -\epsilon_x\bar{A} + (\epsilon_y\bar{B} - \bar{\epsilon}_y B) \tag{10}$$

   deduces the solvability condition

$$\bar{A} = \bar{\delta}\bar{B} - \delta B, \text{where } \bar{\delta} = \epsilon_y/\epsilon_x,\ \delta = \bar{\epsilon}_y/\epsilon_x; 0 \le \sqrt{\delta^2+\bar{\delta}^2} \le 1. \tag{11}$$

4. The Moiseev asymptotic condition

$$\Lambda = \bar{\sigma}_1^2 - 1 = \sigma_1^2/\sigma^2 - 1 = O(\epsilon^{2/3}) \tag{12}$$

   is adopted providing all quantities in (7) are of the equal asymptotic order $O(\epsilon)$.
5. The nondimensional coefficients $m_i = m_i(h)$ are independent of σ, their values were computed in [1] to show that $m_1 > m_2, m_3 > m_2$ as well as $m_3 > m_1, m_3 > 0, m_1 < 0, m_2 < 0$ for $h > 0.3368....$ This and other critical depths leading to zeros for the appearing linear combinations of m_1 are avoided in the analysis.

Even though a uniform periodic tank motion is assumed, the dominant wave contribution (6) is uniquely determined by the first Fourier harmonics of $\eta_i(t)$, the higher Fourier harmonics only influence the $O(\epsilon)$

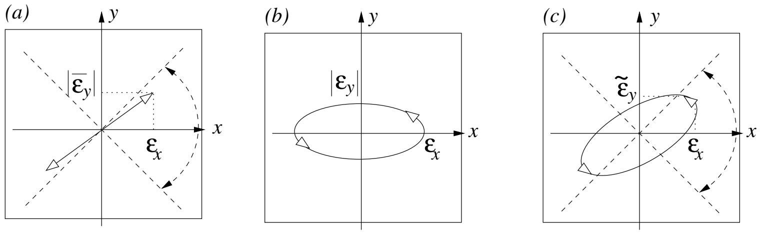

Figure 2. Three schematic trajectories of the equivalent horizontal harmonic tank motions that classify the periodic tank excitations by their first Fourier harmonics (8) with (9). The case (a) implies the *reciprocating* excitation type (longitudinal, diagonal and oblique excitations are particular cases) occurring for $\epsilon_y = 0$. The elliptic excitation type in the case (b) ($\bar{\epsilon}_y = 0$) suggests the major-axis of the ellipse belongs to Ox. The oblique elliptic excitation type in the panel (c) corresponds to $\epsilon_y \bar{\epsilon}_y \neq 0$.

asymptotic terms so that they do not affect the stability of the constructed stead-state solutions. *For any periodic tank motion*, one can introduce an *equivalent harmonic horizontal tank excitation*

$$-P_1 \ddot{\eta}_1^*(t) = \epsilon_x \cos \sigma t; \; -P_1 \ddot{\eta}_2^*(t) = \bar{\epsilon}_y \cos \sigma t + \epsilon_y \sin \sigma t; \; \eta_4^* = \eta_5^* = 0, \quad (13)$$

($P_1 = P_{1,0} = P_{0,1}$) leading to the same equations (7) and, therefore, the periodic solution within to the $O(\epsilon)$ terms. According to (13), the tank moves along the quadratic curve

$$(\varepsilon_y^2 + \bar{\varepsilon}_y^2)\, x^2 + \varepsilon_x^2\, y^2 - 2\varepsilon_x \bar{\varepsilon}_y\, xy = \varepsilon_x^2 \varepsilon_y^2 \;\; (\varepsilon_x = \epsilon_x/P_1, \varepsilon_y = \epsilon_y/P_1, \bar{\varepsilon}_y = \bar{\epsilon}_y/P_1) \quad (14)$$

in the horizontal plane. The curve is either an straight line ($\epsilon_y = 0$) or an ellipse ($\epsilon_y \neq 0$).

We classify the periodic resonant tank excitations by the trajectories (13). The *reciprocating* excitation type with $\epsilon_y = 0$ implies the tank oscillates along an interval in figure 2 (a). The particular cases are longitudinal ($\bar{\epsilon}_y = \epsilon_y = 0$), diagonal ($\epsilon_y = 0$, $|\bar{\epsilon}_y| = \epsilon_x \neq 0$), and oblique ($\epsilon_y = 0$, $0 < |\bar{\epsilon}_y| < \epsilon_x$) excitations. The *elliptic* tank excitation type with $\epsilon_y \neq 0$ is shown in figure 2 (b,c). When $\bar{\epsilon}_y = 0$, the elliptic trajectory possesses the *axisymmetric* shape in figure 2 (b).

The asymptotic steady-state solutions and their *stability* [1] are determined by $A, B, \bar{B}$ ($\bar{A} = \bar{\delta}\bar{B} - \delta B$) which should be analytically found from (7) as functions of Λ (σ/σ_1). The result is the response curves in the *four-dimensional* space $(\sigma/\sigma_1, A, B, \bar{B})$. The main twofold task consists of describing the response curves and, based on (6), classifying the corresponding steady-state wave regimes, which are best characterised by the lowest-order asymptotic wave component

$$z = S(x, y; A, \bar{B}) \cos \sigma t + S(x, y; \bar{\delta}\bar{B} - \delta B, B) \sin \sigma t + o(\epsilon^{1/3}), \qquad (15)$$

where

$$S(x, y; a, b) = (a f_1^{(1)}(x) + b f_1^{(2)}(y)) \qquad (16)$$

is the combined Stokes mode.

According to (15), there are two types of the wave patterns. When $(A, \bar{B})$ and $(\bar{\delta}\bar{B} - \delta B, B)$ are parallel vectors (one of them can be zero), (15) implies a standing resonant wave by a combined Stokes mode. Particular cases are the so-called planar, diagonal and nearly-diagonal (squares-like) steady-state wave regimes specified in [1] for longitudinal and diagonal excitations. Whereas $(A, \bar{B})$ and $(\bar{\delta}\bar{B} - \delta B, B)$ are not parallel, (15) defines a swirling wave, where an almost flat crest travels around each of the four sides with an almost flat trough on the opposite side.

3 The reciprocating excitation type

This excitation type is illustrated by trajectories in figure 2 (a) and, according to (11), it needs

$$\bar{\delta} = 0, \quad \bar{A} = -\delta B, \quad -1 < \delta \le 1 \qquad (17)$$

in (7), $\delta = \tan \alpha$, where α is the angle between the excitation direction and Ox. The lowest-order approximation (15) takes then the form

$$z = S(x, y; A, \bar{B}) \cos \sigma t + B S(x, y; -\delta, 1) \sin \sigma t + o(\epsilon^{1/3}) \qquad (18)$$

where the first combined Stokes mode depends on A and $\bar{B}$.

Standing resonant wave by $S(x, y; A, \bar{B})$. Substituting (17) into ② and ③ of (7) transforms these equations to the form $B\,[...] = 0$. This implies that $B \equiv 0$ is a particular solution, which determines the standing wave by the combined Stokes mode $S(x, y; A, \bar{B})$ where A and $\bar{B}$ should be found from ① and ④ of (7). Because ① takes the form $A\,[...] = \epsilon_x \neq 0$, $A \neq 0$ and the latter two equations ① and ④ can be rewritten in the form

$$\begin{cases} \bar{B}\left[(m_1 - m_2)\bar{B}^2 + (\epsilon_x/A - (m_1 - m_2)A^2)\right] - \delta\epsilon_x = 0, \\ \Lambda = \epsilon_x/A - m_1 A^2 - m_2 \bar{B}^2, \quad m_1 \neq m_2. \end{cases} \qquad (19)$$

The system defines the response curves in the $(\sigma/\sigma_1, A, \bar{B})$ space. The curves can be parametrised by A. The procedure suggests taking $A \neq 0$, solving the depressed cubic with respect to $\bar{B}$ (which has from one to three real roots) and, after getting these roots, computing $\Lambda = \sigma_1^2/\sigma^2 - 1 = \Lambda(A, \bar{B}(A))$.

Longitudinal excitation type. When $\delta = 0$, the depressed cubic in (19) has the zero root $\bar{B} = 0$ and may have the two real roots $\pm|\bar{B}|$ coming from $\bar{B}^2 = \epsilon_x/A/(m_2 - m_1) + A^2 > 0$. The first root implies, according to (18), the so-called planar standing wave by the first Stokes mode, $z = Af_1^{(1)}(x)\cos\sigma t$, but the other two roots imply the so-called nearly-diagonal (squares-like) steady-state wave regimes, which are, in fact, the two standing resonant waves in terms of the combined Stokes modes $S(x, y; A, |\bar{B}|)$ and $S(x, y; A, -|\bar{B}|))$.

Diagonal excitation type. When $\delta = 1$, the depressed cubic in (19) has the real root $\bar{B} = A$ which corresponds to the so-called diagonal steady-state wave (the standing wave by the combined Stokes mode $S(x, y; 1, 1)$). It may also have two real roots coming from the quadratic equation $(m_1 - m_2)(\bar{B}^2 + A\bar{B}) + \epsilon_x/A = 0$. These two roots determine the aforementioned nearly-diagonal (squares-like) steady-state wave regimes.

There are no obvious analytical solutions of the depressed cubic for the *oblique excitation type* with $0 < \delta < 1$ and, therefore, it should be solved numerically. The number of real roots depends on the discriminant

$$\Delta_1(A) = -(m_1 - m_2)\left[4\left(\frac{\epsilon_x}{A} - (m_1 - m_2)A^2\right)^3 + 27(m_1 - m_2)\delta^2\epsilon_x^2\right]. \quad (20)$$

When $\Delta_1 > 0$, the depressed cubic has three different real roots, the case $\Delta_1 = 0$ implies two real roots one of which has the double multiplicity, and, finally, the negative discriminant causes only one real root.

Swirling. When $B \neq 0$, one can divide (10) by B and, provided by (17), express ④ through ①, ② and ③. These three equations can, after tedious derivations, be rewritten in the form

$$\delta^2\bar{B}^3 + \delta A(2 - \delta^2)\bar{B}^2 + A^2(1 - 2\delta^2)\bar{B} + \delta\left[\epsilon_1(1 - \delta^2) - A^3\right] = 0,$$
$$\epsilon_1 = \frac{\epsilon_x(m_2 - m_1)}{(m_2 - m_3)(m_1 - m_3)}, \quad (21a)$$

$$B^2 = \frac{A\left[(m_1 - m_3)A^2 + (m_2 - m_1)\bar{B}^2 + \delta(m_2 - m_3)A\bar{B}\right] - \epsilon_x}{\delta(m_2 - m_3)\bar{B} + (m_1 - m_3 + \delta^2(m_2 - m_1))A} > 0, \quad (21b)$$

$$\Lambda = \epsilon_x/A + \delta(m_2 - m_3)\bar{B}B^2/A - m_1A^2 - m_2\bar{B}^2 - (m_3 + \delta^2 m_1)B^2. \quad (21c)$$

The expressions assume that $A \neq 0$ along a response curve (the fact can be proved) and the denominator $\delta(m_2-m_3)\bar{B}+(m_1-m_3+\delta^2(m_2-m_1))A$ is not zero as well.

The formulas (a), (b) and (c) in (21) consequently determine an analytical solution and the response curves in the *four-dimensional* space $(\sigma/\sigma_1, A, \bar{B}, |B|)$ parametrically defined by A: by taking a real $A \neq 0$, we solve the cubic equation (21a) with respect to $\bar{B}$ (analytically, by using Cardano's formulas, or numerically), compute $\pm|B|$ (if exist) by (21b) and Λ (the forcing frequency ratio σ/σ_1) by (21c). The cubic equation equation (21a) may have from three to one real number that depends on the discriminant

$$\Delta_2(A) = -\epsilon_1\delta^4(\delta^2 - 1)[27\epsilon_1\delta^2(\delta^2 - 1) + 4A^3(\delta^2 + 1)^3], \quad (22)$$

which is identical to zero for longitudinal ($\delta = 0$) and diagonal ($|\delta| = 1$) excitations. The analytical solution (21) transforms to a standing wave when the vectors $(A, \bar{B})$ and $(-\delta, 1)$ are parallel ($A = -\delta\bar{B}$). Substituting $A = -\delta\bar{B}$ into (21a) leads to $\delta\epsilon_1(1-\delta^2) = 0$ which, again, is only possible for the two limit cases $\delta = 0$ and $|\delta| = 1$.

Longitudinal excitation type. When $\delta = 0$, (17) $\Rightarrow \bar{A} = 0$ and (21a) $\Rightarrow \bar{B} = 0$. Remaining A, B and Λ are governed by (21b) and (21c) which are equivalent to the relationships in [1]. This solution is the swirling steady-state wave regime by the Stokes modes $f_1^{(1)}(x)$ and $f_1^{(2)}(y)$ which may occur in the two opposite directions due to $B = \pm|B|$ in (18).

Diagonal excitation type. When $\delta = 1$, the cubic equation (21a) has, according to $\Delta_2 \equiv 0$, two real roots. The root of the single multiplicity is $\bar{B} = A$ but the root $\bar{B} = -A$ has the double multiplicity. The first root determines swirling by the two perpendicular combined Stokes modes $S(x, y; 1, 1)$ and $S(x, y; -1, 1)$ which can also occur into two different directions since B is defined within to the sign. The root $\bar{B} = -A$ is mathematically impossible as leading to $B^2 \cdot 0 = A \cdot 0 - \epsilon_x \neq 0$ in (21b).

4 The axisymmetric elliptic excitation type

This excitation type is associated with the elliptic trajectory of the equivalent horizontal tank motions in figure 2 (a). Mathematically, this implies $\bar{\epsilon}_y = \delta\epsilon_x = 0$ in (7) so that (11) leads to

$$\bar{A} = \bar{\delta}\bar{B}, \quad 0 < \bar{\delta} \leq 1. \quad (23)$$

Without less of generality, the counterclockwise direction along the elliptic orbit is chosen. The limit case $\bar{\bar{\delta}} = 1$ corresponds to the rotary (circular) excitation type. The lowest-order asymptotic approximation (15) gives

$$z = S(x, y; A, \bar{B}) \cos \sigma t + S(x, y; \bar{\bar{\delta}}\bar{B}, B) \sin \sigma t + o(\epsilon^{1/3}) \tag{24}$$

in terms of the two combined Stokes modes.

Swirling by the two Stokes modes. Substituting (23) into (7) transforms ③ and ④ to the form $\bar{B}[...] = 0$ that means that $\bar{A} = \bar{B} = 0$ is a particular solution of the secular system. The two non-zero amplitude parameters A and B can be found from ① and ② rewritten in the form

$$\begin{cases} B\left[(m_1 - m_3)B^2 + (\epsilon_x/A - (m_1 - m_3)A^2)\right] - \bar{\bar{\delta}}\epsilon_x = 0, \ A \neq 0, \\ \Lambda = \epsilon_x/A - m_1 A^2 - m_3 B^2, \end{cases} \tag{25}$$

which gives an analytical solution and the corresponding response curves in the space $(\sigma/\sigma_1, A, B)$ parametrically defined as functions of A. The procedure suggests solving the depressed cubic which may have from one to three real roots depending on the discriminant

$$\Delta_3(A) = -(m_1 - m_3)\left[4\left(\frac{\epsilon_x}{A} - (m_1 - m_3)A^2\right)^3 + 27(m_1 - m_3)\bar{\bar{\delta}}^2\epsilon_x^2\right]. \tag{26}$$

Because $\bar{A} = \bar{B} = 0$, (24) defines the steady-state swirling by the Stokes modes $f_1^{(1)}(x)$ and $f_1^{(2)}(y)$. The signs of A and B are determined by (25) and, therefore, the swirling direction is defined as well.

Passage to the longitudinal excitation type. When $\bar{\bar{\delta}} \to 0$, the elliptic orbit in figure 2 (a) flattens and this excitation type transforms to the longitudinal excitations along the Ox axis. In this limit, the depressed cubic has the real root $B = 0$ which implies the planar steady-state wave regime. The two other real roots $\pm|B|$ are computed by $B^2 = \epsilon_x/A/(m_3 - m_1) + A^2 > 0$; these define two swirling waves whose direction depends on the transients stage.

The rotary excitation with $\bar{\bar{\delta}} = 1$. The depressed cubic in (25) has then the real root $B = A$ which corresponds to the co-called rotary (swirling) wave. The two other real roots come from the quadratic equation $(m_1 - m_3)(B^2 + AB) + \epsilon_x/A = 0$ with respect to B.

Swirling by the two combined Stokes modes. When $\bar{B} \neq 0$, dividing (10) by $\bar{B}$ makes it possible to express ② via ①, ③ and ④. These three equations can be rewritten in the form

$$\bar{\delta}^2 B^3 + \bar{\delta} A(2-\bar{\delta}^2)B^2 + A^2(1-2\bar{\delta}^2)B + \bar{\delta}\left[\epsilon_2(1-\bar{\delta}^2) - A^3\right] = 0,$$
$$\epsilon_2 = \frac{\epsilon_x(m_3-m_1)}{(m_2-m_3)(m_2-m_1)}, \quad (27a)$$

$$\bar{B}^2 = \frac{A\left[(m_2-m_1)A^2 + (m_1-m_3)B^2 + \bar{\delta}(m_2-m_3)AB\right] + \epsilon_x}{\bar{\delta}(m_2-m_3)B + (m_2-m_1+\bar{\delta}^2(m_1-m_3))A} > 0, \quad (27b)$$

$$\Lambda = \epsilon_x/A - \bar{\delta}(m_2-m_3)\bar{B}^2B/A - m_1A^2 - m_3B^2 - (m_2+\bar{\delta}^2 m_1)\bar{B}^2, \quad (27c)$$

which defines the analytical solution and the response curves in the space $(\sigma/\sigma_1, A, B, |\bar{B}|)$ (parametrised by $A \neq 0$). The equation (27) has from one to three real roots depending on the discriminant

$$\Delta_4(A) = -\epsilon_2\bar{\delta}^4(\bar{\delta}^2-1)[27\epsilon_2\bar{\delta}^2(\bar{\delta}^2-1) + 4A^3(\bar{\delta}^2+1)^3]. \quad (28)$$

The solution (27) implies the swirling steady-state wave regime by the two combined Stokes modes (24) which becomes a standing resonant wave by a combined Stokes wave when $\bar{\delta}\bar{B} = AB$ (the two vectors $(A, \bar{B})$ and $(\bar{\delta}\bar{B}, B)$ are parallel). Requiring this condition in (27b) deduces the algebraic algebraic equation

$$-\bar{A}^3 + AB[\bar{\delta}B + (1-\bar{\delta}^2)A^2] - \frac{\bar{\delta}\epsilon_x}{m_2-m_1} = 0, \quad AB > 0, \ 0 < \delta \leq 1, \quad (29)$$

which constitutes, together with (27a), an algebraic system to find (A, B) for which (24) implies the standing wave.

Passage to the longitudinal reciprocating excitation. When $\bar{\delta} \to 0$, $\bar{A} = 0$ from (23) and $B = 0$ from (27a). The two equations, (27c) and (27b), describe the two standing squares-like resonant waves, $z = [Af_1^{(1)}(x) \pm |\bar{B}|f_1^{(2)}(y)]\cos\sigma t + o(\epsilon^{1/3})$, which were described in [1].

The rotary excitation type implies $\bar{\delta} = 1$ in (27). The two real roots of (27a) are $B = A$ and $B = -A$ (of the double multiplicity, $\Delta_4 \equiv 0$ as $\bar{\delta} = 1$). The second root contradicts to (27b) as causing $\bar{B}^2 \cdot 0 = A \cdot 0 + \epsilon_x \neq 0$, but $B = A \neq 0$ in (27b) and (27c) leads to the steady-state swirling by the combined Stokes modes (24), where

$$\Lambda = -2(m_1+m_2-m_3)A^2 + \epsilon_x(1-m_2-2m_2+m_3)/A, \quad A \neq 0 \quad (30)$$

provided by $B = A, \bar{B}^2 = A^2 + \epsilon_x/A > 0$, $(m_1+m_2-m_3) \neq 0$ and $(1-m_1-2m_2+m_3) \neq 0$.

5 The oblique elliptic excitation type

When all forcing amplitudes in (7) are not zeros, $\epsilon_x\,\epsilon_y\,\bar\epsilon_y \neq 0$, the first Fourier harmonic component of the periodic tank excitations determines an oblique elliptic orbit in figure 2 (c) in terms of the equivalent horizontal tank motions. The equation (11) contains both non-zero coefficients,

$$\bar A = \bar\delta \bar B - \delta B, \quad \delta\,\bar\delta \neq 0. \tag{31}$$

The amplitude parameter $\bar A \neq 0$ since assuming the zero transforms (7) to the contradiction $A\bar B B = 0, A[...] = \epsilon_x \neq 0, \bar B[...] = \epsilon_y \neq 0, B[...] = \bar\epsilon_y \neq 0$. This means that dividing (10) by $\bar A \neq 0$ makes ① derivable from other three secular equations as (31) is satisfied.

Moreover, whereas $\delta\bar\delta \neq 0$, $A\bar B B \not\equiv 0$ along a response curve. A tedious derivation reduces finding the semi-analytical solution to getting real roots of

$$\sum_{i=0}^{9} c_i^{(0)} B^i \bar B^{9-i} + \epsilon_3 \sum_{i=0}^{6} c_i^{(1)} B^i \bar B^{6-i} + \epsilon_3^2 \sum_{i=0}^{3} c_i^{(2)} B^i \bar B^{3-i} = 0;\ \epsilon_3 = \frac{\epsilon_x}{m_2 - m_3}, \tag{32}$$

where coefficients $c_i^{(0)}, c_i^{(1)}$ and $c_i^{(2)}$ are the polynomials by $\delta, \bar\delta$ and the quadratic functions by m_1, m_2 and m_3. The equality (32) can be considered as, for instance, an algebraic equation with respect of B when $\bar B \neq 0$ is a real parameter. At least one real root must exist. After getting all real roots of (32), (31) computes $\bar A$ but the following formulas consequently compute A and σ/σ_1,

$$\begin{aligned} A = -\bar A \big[& \epsilon_3(\delta B m_3 - \bar\delta \bar B m_2 + m_1 \bar A) \\ & + B\bar B((m_1 - m_2)B^2 + (m_1 - m_3)\bar B^2 + (m_2 + m_3)\bar A^2)\big] \\ & / \left[\bar A^2((m_2 - m_1)\bar B^2 - (m_3 - m_1)B^2] + B^2 \bar B^2 (m_2 - m_3)\right], \end{aligned} \tag{33a}$$

$$\Lambda = -m_1(A^2 + \bar A^2) - m_2 B^2 - m_3 \bar B^2 - (m_2 - m_3) A B \bar B / \bar A. \tag{33b}$$

As a consequence, changing $\bar B \neq 0$, (32), (31) and (33) determine from one to nine response curves in the space $(\sigma/\sigma_1, A, \bar B, B)$.

This semi-analytical solution defines the steady-state resonance wave patterns (15). They imply a swirling wave in the most general case but it can also imply a standing wave when the vector $(A, \bar B)$ and $(\bar\delta \bar B - \delta B, B)$ are parallel, namely, when the condition

$$AB = \bar B(\bar\delta \bar B - \delta B) \tag{34}$$

is satisfied.

6 Conclusions

Using the Narimanov-Moiseev approximate modal theory for the resonant sloshing in a square-base tank, we study the steady-state wave regimes occurring due to a periodic small-magnitude sway-surge-roll-pitch motion of the tank. The only first Fourier harmonics of the periodic forcing matters for classifying the resonant steady-state surface waves. This makes it possible to introduce an equivalent horizontal harmonic tank forcing, which causes the same steady-state resonant waves in terms of the first and second asymptotic components. This equivalent forcing can be identified as of either reciprocating or elliptic type.

The analytical solutions for the reciprocating and elliptic excitation types are constructed. Existence of standing and swirling wave regimes in certain frequency ranges is confirmed. For the elliptic excitation type, only swirling-type waves are theoretically possible.

[1] *Faltinsen O.M., Rognebakke O.F., Timokha A.N.* Resonant three-dimensional nonlinear sloshing in a square base basin // Journal of Fluid Mechanics. — 2003. — **487**. — P. 1–42.

[2] *Faltinsen O. M., Rognebakke O. F., Timokha A. N.* Resonant three-dimensional nonlinear sloshing in a square base basin. Part 2. Effect of higher modes // Journal of Fluid Mechanics. — 2005. — **523**. — P. 199–218.

[3] *Faltinsen O. M., Rognebakke O. F., Timokha A. N.* Resonant three-dimensional nonlinear sloshing in a square base basin. Part 3. Base ratio perturbations // Journal of Fluid Mechanics. — 2006. — **551**. — P. 93–116.

[4] *Faltinsen O. M., Rognebakke O. F., Timokha A. N.* Transient and steady-state amplitudes of resonant three-dimensional sloshing in a square base tank with a finite fluid depth // Physics of Fluids. — 2006. — **18**, Art. No. 012103. — P. 1–14.

[5] *Faltinsen O. M., Timokha A. N.* Sloshing. — Cambridge University Press, 2009. — 686 p.

[6] *Ikeda T., Harata Y., Osasa T.* Internal resonance of nonlinear sloshing in rectangular liquid tanks subjected to obliquely horizontal excitation // Journal of Sound and Vibration. — 2016. — **361**. — P. 210–225.

[7] *Ikeda T., Ibrahim R. A., Harata Y., Kuriyama T.* Nonlinear liquid sloshing in a square tank subjected to obliquely horizontal excitation // Journal of Fluid Mechanics. — 2012. — **700**. — P. 304–328.

[8] *Pilipchuk V. N.* Nonlinear interactions and energy exchange between liquid sloshing modes // Physica D. — 2013. — **263**. — P. 21–40.

[9] *Wu Chih-Hua, Chen Bang-Fuh* Sloshing waves and resonance modes of fluid in a 3D tank by a time-independent finite difference method // Ocean Engineering. — 2009. — **36**.— P. 500–510.

[10] *Wu Chih-Hua, Chen Bang-Fuh, Hung Tin-Kan* Hydrodynamic forces induced by transient sloshing in a 3d rectangular tank due to oblique horizontal excitation // Computers and Mathematics with Applications. — 2013. — **65**. — P. 1163–1186.

[11] *Wu Chih-Hua, Faltinsen O.M., Chen Bang-Fuh* Analysis on shift of nature modes of liquid sloshing in a 3d tank subjected to oblique horizontal ground motions with damping devices // Advances in Mechanical Engineering. — 2013. — Article ID 627124. — P. 1-24.

[12] *Zhang Hong-Shang, Wu Peng-Fei, Liu Wen-Bai* The analysis of second-order sloshing resonance in a 3-D tank // Journal of Hydrodynamics. — 2014. — **26**, no. 2. — P. 309-315.